Analyst

Cite this: *Analyst*, 2011, **136**, 1686

www.rsc.org/analyst

PAPER

Vapor–liquid–solid grown silica nanowire based electrochemical glucose biosensor

Eduardo Murphy-Pérez, Sunil K. Arya* and Shekhar Bhansali*

Received 6th December 2010, Accepted 8th February 2011
DOI: 10.1039/c0an00977f

Vapor–liquid–solid (VLS) grown silica nanowires (SiO_2NWs) have been deposited electrophoretically on a gold electrode and utilized for covalent immobilization of glucose oxidase (GOx). Covalent binding has been achieved *via* 3-aminopropyltriethoxysilane (APTES) modification and *N*-ethyl-*N*′-(3-dimethylaminopropyl) carbodiimide and *N*-hydroxysuccinimide chemistry. Scanning electron microscopy, transmission electron microscopy and cyclic voltammetry techniques have been used to characterize SiO_2NW and GOx/APTES/SiO_2NW/Au bioelectrode. Electrochemical studies reveal that SiO_2NW increases the effective electro-active surface area thus resulting in higher loading of enzyme. Response characteristics show linearity in the range of interest 25–300 mg dl^{-1}, with a detection limit of 11 mg dl^{-1}, sensitivity: 0.463 μA (mg dl^{-1})$^{-1}$ and regression coefficient of 0.992.

1. Introduction

Electrochemical biosensors possessing high accuracy, sensitivity and cost-effectiveness continue to be a technology of interest in clinical diagnostics.[1–3] Integrating affordable nanomaterials with chemically tailored physicochemical properties enables improvement in sensitivity while reducing cost.[4–6] Among nanomaterials, oxides such as ZnO, CeO_2, ZrO_2 and SiO_2 are potential candidates that have recently gained much attention due to high surface-to-volume ratio, high surface reaction activity, and ease of preparation.[7–10] Sol–gel based silica (SiO_2) films have shown biocompatibility and high stability as a matrix material. SiO_2 nanowires (SiO_2NWs) have offered greater versatility due to their unique anisotropy in physical, optical, electronic properties with excellent photoluminescence and biocompatibility.[11,12] Further, SiO_2NWs' surface can be easily and effectively modified with standard silane based chemistries.[13] However, their growth and optimal deposition of SiO_2NWs on the surface of an electrode had proven to be a challenge that needed exploring.

There are many different techniques to synthesize semiconductor nanowires, however, the vapor–liquid–solid (VLS) process is most common for fabrication of semiconductor nanowires.[14] VLS is a bottom-up method where metals like gold, palladium, platinum *etc.* react with the silicon substrate to form silicide islands that are dispersed on a Si substrate. The vapor phases dissolve in these silicide and nanowires precipitate out of the super saturated silicide. Using VLS, it is possible to grow nanowires with controlled diameters.[14] Recently, Sood *et al.*[15] have described a method for selective growth of SiO_2NWs on silicon wafers using palladium ion implantation. They have shown that Pd nanoclusters get activated and act as catalyst silicide seeds for selective nanowire growth on the implanted region, when heated in an open tube quartz furnace, using Ar as carrier gas. They have also suggested their applications in on-chip optoelectronics, biosensors and microantennae. Sekhar *et al.*[16] have described the selective growth of amorphous silica nanowires on a silicon wafer deposited with Pt thin film. They have established the mechanism of nanowire growth and suggested that it follows the vapour–liquid–solid (VLS) model *via* the PtSi phase acting as the catalyst. Using this bottom-up technique they were able to grow nanowires with diameters ranging from 50 to 500 nm. Later, they have described the selective growth of silica nanowires using an Au catalyst for optical recognition of interleukin-10.[17] In the present work, an attempt has been made to utilize these biocompatible silica nanowires selectively grown using palladium implant for biosensor fabrication.

The VLS method results in growth of dense nanowires akin to a bed of grass and weeds. Approaches for their dispersion in a suitable solvent and deposition on a metallic surface for electrochemical biosensor fabrication are still being optimized. Recently, electrophoretic deposition (EPD) of nanostructures including nanowires has been shown to result in uniform and densely packed structures with controlled thickness and morphology.[18,19] EPD is commonly employed in processing and deposition of ceramics, coatings, composite materials, carbon nanotubes and conducting polymers. It is achieved *via* motion of charged particles, dispersed in a suitable solvent, towards an electrode under an applied electric field. Deposition on the electrode occurs *via* particle coagulation. Electrophoretic

Bio-MEMS and Microsystem Lab, Department of Electrical Engineering, University of South Florida, Tampa, FL, 33620, USA. E-mail: sunilarya333@gmail.com; bhansali@usf.edu; Fax: +1-813-974-5250; Tel: +1-813-97407942

motion of charged particles during EPD results in the accumulation of particles and the formation of films or coatings with good microstructure homogeneity and high packing density from colloidal suspensions.[20–24] EPD has the advantage of simplicity, cost-effectiveness, simple equipment requirement, amenability to scaling-up to large dimensions and applicability to a great variety of materials. Recently, Dhand *et al.* have described application of EPD for deposition of polyaniline film[25] and multiwalled carbon nanotubes (MWCNT-c)[26] on indium-tin-oxide (ITO) coated glass plate and shown that EPD results in smoother and uniform morphology for the deposited film in comparison to the electrochemically deposited films.

In this manuscript, we report the application of electrophoretically deposited VLS grown SiO_2NWs for fabrication of electrochemical enzymatic biosensor. SiO_2NWs were electrophoretically deposited, and modified with 3-aminopropyltriethoxysilane (APTES) for covalent immobilization of glucose oxidase (GOx) as model enzyme. The GOx/APTES/SiO_2NWs/Au bioelectrode fabricated in this way has been found to be sensitive to glucose, with high sensitivity of 0.463 μA (mg $dl^{-1})^{-1}$.

2. Materials and methods

2.1. Silica nanowire growth and bioelectrode fabrication

All chemicals of analytical grade were purchased from Sigma Aldrich. As reported earlier by our group, SiO_2NWs were grown using a metal seeded vapor–liquid–solid (VLS) mechanism.[10] In brief, palladium (Pd) ions were implanted into Si(100) and then annealed at 1100 °C in Ar environment to grow nanowires. For electrophoretic deposition on gold surface, a stock solution of SiO_2NW (~0.4 mg ml^{-1}) was prepared in 10 mM $NiCl_2 \cdot 6H_2O$ through sonication and then 40 μl of the solution was aliquoted and dispersed in 2 ml of acetonitrile through sonication. Nanowire deposition was then carried out using a cell with two electrodes, placed parallel to each other with separation of 1 cm and by applying DC voltage (100 V) for 60 s. The electrode, now modified with SiO_2NWs, was washed with water and silanized using 2% APTES in methanol for 2 h which resulted in a large number of amino groups on NW surface. The GOx was covalently attached to APTES amino groups using *N*-ethyl-*N*′-(3-dimethylaminopropyl)carbodiimide and *N*-hydroxysuccinimide (EDC/NHS) chemistry. The quantity of enzyme used was optimized and 30 μl of 2 mg ml^{-1} GOx solution in PBS containing 0.4 M EDC and 0.1 M NHS were used. The enzyme solution was poured onto APTES modified NW surface (0.25 cm^2) and incubated for 2 h at room temperature for GOx binding. The electrode (GOx/APTES/SiO_2NW/Au) formed was washed thoroughly with phosphate buffer (10 mM, pH 7.0) containing 0.9% NaCl to remove any unbound enzyme. The electrode was stored at 4 °C when not in use. Fig. 1 shows the schematic for GOx/APTES/SiO_2NW/Au bioelectrode fabrication.

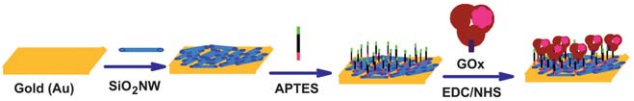

Fig. 1 Schematic for GOx/APTES/SiO_2NW/Au bio-electrode fabrication.

2.2. Measurement and apparatus

TEM characterization and SEM studies were conducted using FEI Tecnai™ SEM & TEM to characterize nanowires and electrode formation. Cyclic voltammetric studies, using an Autolab Potentiostat/Galvanostat from Autolab, were done to characterize electrode fabrication, concentration studies and electrochemical studies. CV studies were carried out in phosphate buffer saline (PBS) 10 mM, pH 7.5 containing 0.1 mM $Fe(CN)_6^{3-/4-}$ in the electrode cell with Ag/AgCl as reference electrode and gold film as counter electrode.

3. Results and discussion

3.1. SEM and TEM characterization

Fig. 2 shows the SEM image of GOx modified electrode where globular kind of structures represent the bound GOx on SiO_2NWs. The inset shows the TEM image of VLS grown SiO_2NW revealing the presence of pure SiO_2NW with a diameter of 20 to 70 nm.

3.2. Cyclic voltammetric characterization

Fig. 3 shows the cyclic voltammograms obtained from different modified electrodes. The increase in the oxidation current of the SiO_2/Au (curve (ii)) on gold plate compared to that of the Au electrode (curve (i)) indicates the deposition of SiO_2NW that results in formation of a three dimensional surface electrode with larger surface area compared to a plain Au surface. Further, the increase in current is attributed to the use of 10 mM $NiCl_2 \cdot 6H_2O$ solution as charger salt for dispersion and deposition of silica nanowires on a negative electrode. The interaction of $NiCl_2 \cdot 6H_2O$ solution with silica nanowires also results in deposition of Ni particles on the surface of the silica nanowires. EDAX studies confirm the presence of nickel on the surface (data not shown). Thus formation of the three dimensional surface electrode with a larger surface area and the presence of nickel on the surface result in an increase of redox probe ($Fe(CN)_6^{3-/4-}$) current in the diffusion controlled process. In curve (iii) the increase in current for APTES/SiO_2NW/Au suggests the APTES

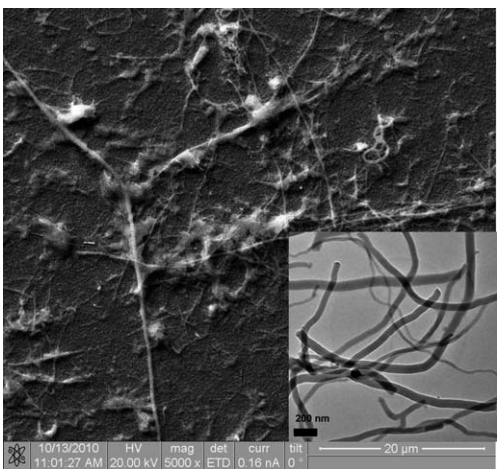

Fig. 2 SEM image of GOx modified electrode. Inset: TEM image of VLS grown SiO_2NW.

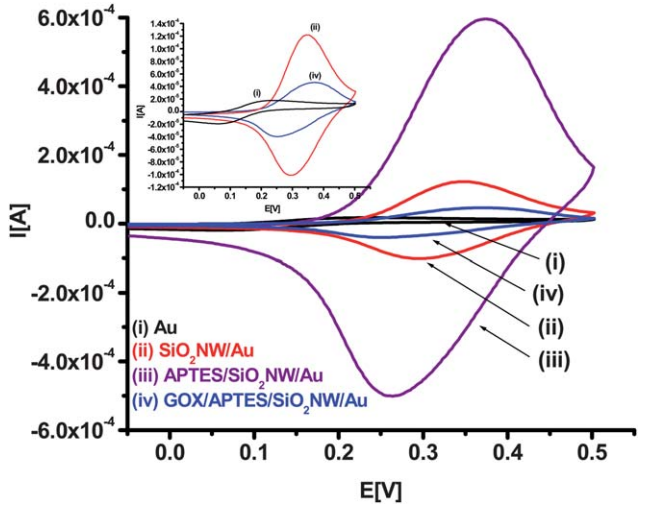

Fig. 3 CV characterization of GOx/APTES/SiO_2NW/Au bio-electrode fabrication in phosphate buffer saline (PBS) 10 mM, pH 7.5 containing 0.1 mM $Fe(CN)_6^{3-/4-}$ at 50 mV s^{-1}.

SAM formation which results in the generation of a large number of polarizable amino groups on the surface. The presence of possible positive charge on the amino groups attracts the negatively charged redox probe towards the electrode surface and facilitates redox behavior of $Fe(CN)_6^{3-/4-}$ at the surface.[27] After GOx binding (curve (iv)), a decrease in current response was observed and is attributed to the insulating and macromolecular structure of the GOx molecule that hinders the electron transfer.

3.3. Scan rate studies

Fig. 4a shows the CV studies of SiO_2/Au electrode at different scan rates ranging from 10 to 100 mV s^{-1}. It is clear from Fig. 4a that the magnitude of current response increases with increasing scan rate and exhibits a linear relationship with square root of scan rate (inset of Fig. 4a), suggesting a diffusion controlled process. Furthermore, the quasi reversible curves and observed linear dependence of potential difference as a function of scan rate reveal the facile electron transfer.[28] These studies suggest that the SiO_2NW based matrices can provide a useful matrix for electrochemical biosensors.

Fig. 4b shows the scan rate response for the GOx/APTES/SiO_2NW/Au bio-electrode. It can be seen that after binding of GOx on APTES modified SiO_2 the oxidation current decreases and the oxidation peak potential shifted to a higher value suggesting formation of a diffusion inhibiting insulating layer on the electrode surface. However, well defined quasi reversible peaks even after GOx deposition reveal the advantage of SiO_2NW's for matrix application. Further, the linear relationship between magnitude of the current response and square root of scan rate (inset of Fig. 4b), suggests a diffusion controlled process on the GOx/APTES/SiO_2NW/Au bio-electrode.

3.4. Glucose concentration studies

Fig. 5 shows the CV spectra of GOx/APTES/SiO_2NW/Au for various glucose concentrations. It is observed that the magnitude

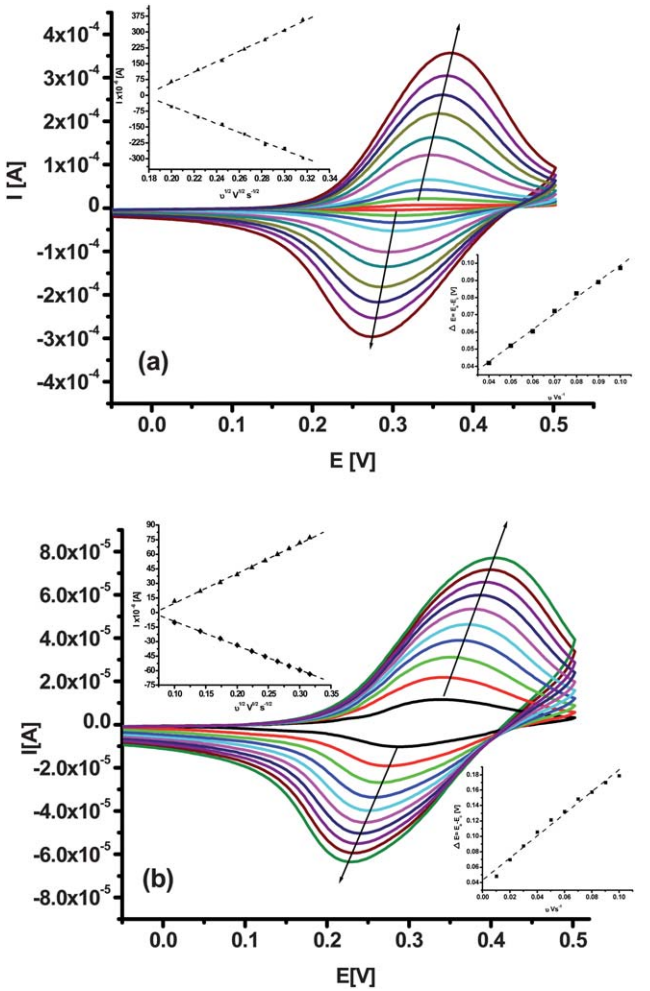

Fig. 4 Scan rate studies of (a) SiO_2NW/Au and (b) GOx/APTES/SiO_2NW/Au bio-electrode.

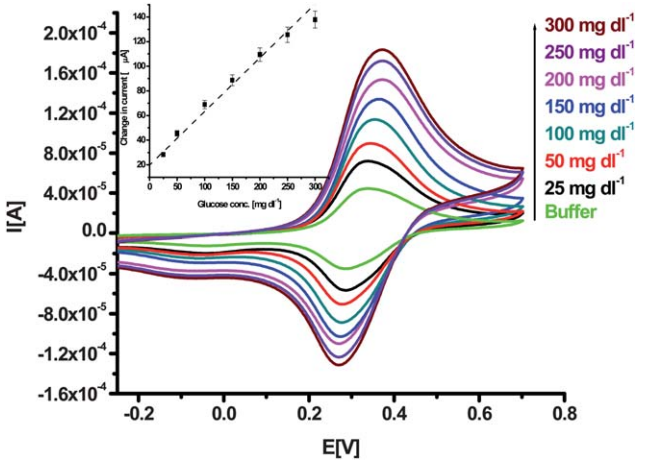

Fig. 5 CV spectra of GOx/APTES/SiO_2NW/Au for (i) buffer, (ii) 25 mg dl^{-1}, (iii) 50 mg dl^{-1}, (iv) 100 mg dl^{-1}, (v) 150 mg dl^{-1}, (vi) 200 mg dl^{-1}, (vii) 250 mg dl^{-1} and (viii) 300 mg dl^{-1} of glucose concentration in phosphate buffer saline (PBS) 10 mM, pH 7.5 containing 0.1 mM $Fe(CN)_6^{3-/4-}$ at 50 mV s^{-1}. Inset: linearity curve for various glucose concentrations. Results of triplicate sets are indicated by error bars.

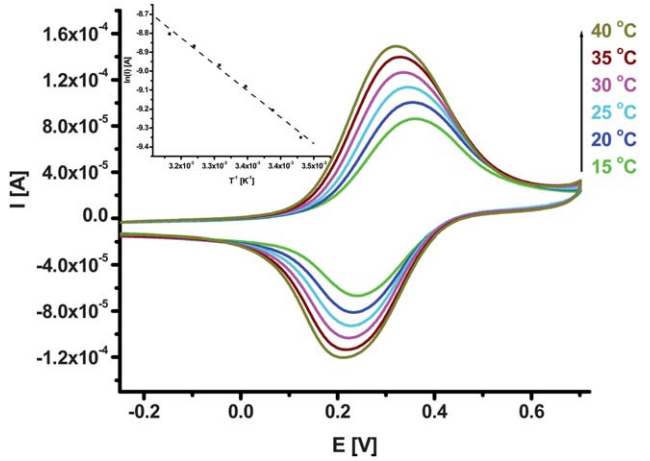

Fig. 6 Temperature response studies of GOx/APTES/SiO_2NW/Au bio-electrode for 100 mg dl^{-1} glucose in phosphate buffer saline (PBS) 10 mM, pH 7.5 containing 0.1 mM $Fe(CN)_6^{3-/4-}$ at 50 mV s^{-1}. Inset: Arrhenius plot, curve between inverse of absolute temperature and ln (*I*).

of the electrochemical response current of the GOx/APTES/SiO_2NW/Au electrode increases with increasing concentration of glucose (Fig. 5). It is attributed to enzymatic catalytic action of GOx bound on the SiO_2NW surface that acts as a high surface area matrix and facilitates higher electron transfer rate. A linear relationship (inset, Fig. 5) between magnitude of current and glucose concentration has been observed and follows I (μA) = 19.744 (μA) + 0.4359 (μA (mg $dl^{-1})^{-1}$) Glu. Conc. (mg dl^{-1}), with a detection limit of 11 mg dl^{-1}, a standard deviation of 1.60 μA and $R^2 = 0.99157$. A high sensitivity of 0.4359 (μA (mg $dl^{-1})^{-1}$) indicates high loading of GOx on a larger surface area and faster electron transfer provided by SiO_2NWs.

3.5. Temperature and interferent studies

Temperature studies between 15 and 40 °C (Fig. 6) show gradually increasing current response for 100 mg dl^{-1} glucose concentration, revealing a high thermal stability for immobilized enzyme with a low activation energy (E_a) of 16.56 kJ mol^{-1} calculated from the Arrhenius plot (inset, Fig. 6). Interferent studies and pH studies (pH 6.0 to 8.0) (data not shown) indicate that electrodes work best at pH 7.0 and are selective against urea (0.5 mM) and ascorbic acid (0.25 mM).

4. Conclusions

In summary, SiO_2NW provides a biocompatible matrix and increases the electroactive surface area of the electrode for the immobilization of GOx, thus resulting in enhanced electron transport and a high sensitivity of 0.4359 (μA (mg $dl^{-1})^{-1}$). Electrophoretically deposited SiO_2NW represents a new biosensor platform for the sensitive detection of glucose and may find potential application for detection of other clinically important analytes such as cholesterol and urea, among others.

Acknowledgements

This work was supported through NSF award 0700659; Nano-engineered, Manufacturable, Ion-Implantation Seeded Silica Nanowires for Sensitive BioScreening. Authors are thankful to Eric Huey and Dr Subramaniam Krishnan for growing silica nanowires. EMP is thankful to Dr Bernard Batson for support and valuable suggestions.

References

1 J. Wang, *Chem. Rev.*, 2008, **108**, 814–825.
2 S. K. Arya, A. Chaubey and B. D. Malhotra, *Proc. Indian Natl. Sci. Acad.*, 2006, **72**, 249–266.
3 O. A. Sadik, A. O. Aluoch and A. L. Zhou, *Biosens. Bioelectron.*, 2009, **24**, 2749–2765.
4 P. Pandey, M. Datta and B. D. Malhotra, *Anal. Lett.*, 2008, **41**, 159–209.
5 C. Jianrong, M. Yuqing, H. Nongyue, W. Xiaohua and L. Sijiao, *Biotechnol. Adv.*, 2004, **22**, 505–518.
6 X. J. Huang and Y. K. Choi, *Sens. Actuators, B*, 2007, **122**, 659–671.
7 M. Vafaee and M. S. Ghamsari, *Mater. Lett.*, 2007, **61**, 3265–3268.
8 L. Li and Y. S. Chen, *Mater. Sci. Eng., A*, 2005, **406**, 180–185.
9 X. L. Liu, D. L. Cui, Q. Wang, Y. Li and Y. Guo, *Mater. Chem. Phys.*, 2007, **105**, 208–212.
10 P. K. Sekhar and S. Bhansali, *Mater. Lett.*, 2010, **64**, 729–732.
11 R. Q. Zhang, Y. Lifshitz and S. T. Lee, *Adv. Mater.*, 2003, **15**, 635–640.
12 F. Patolsky, G. Zheng and C. M. Lieber, *Nanomedicine*, 2006, **1**, 51–65.
13 S. Aravamudhan, N. S. Ramgir and S. Bhansah, *Sens. Actuators, B*, 2007, **127**, 29–35.
14 V. Schmidt and U. Gosele, *Science*, 2007, **316**, 698–699.
15 D. K. Sood, P. K. Sekhar and S. Bhansali, *Appl. Phys. Lett.*, 2006, **88**, 143110.
16 P. K. Sekhar, S. N. Samhandam, D. K. Sood and S. Bhansali, *Nanotechnology*, 2006, **17**, 4606–4613.
17 P. K. Sekhar, N. S. Ramgir, R. K. Joshi and S. Bhansali, *Nanotechnology*, 2008, **19**, 245502.
18 P. Lommens, D. Van Thourhout, P. F. Smet, D. Poelman and Z. Hens, *Nanotechnology*, 2008, **19**, 245301.
19 I. Corni, M. P. Ryan and A. R. Boccaccini, *J. Eur. Ceram. Soc.*, 2008, **28**, 1353–1367.
20 O. O. Van der Biest and L. J. Vandeperre, *Annu. Rev. Mater. Sci.*, 1999, **29**, 327–352.
21 P. Sarkar and P. S. Nicholson, *J. Am. Ceram. Soc.*, 1996, **79**, 1987–2002.
22 A. R. Boccaccini and I. Zhitomirsky, *Curr. Opin. Solid State Mater. Sci.*, 2002, **6**, 251–260.
23 A. R. Boccaccini, J. Cho, J. A. Roether, B. J. C. Thomas, E. J. Minay and M. S. P. Shaffer, *Carbon*, 2006, **44**, 3149–3160.
24 C. Dhand and B. D. Malhotra, in *Organic Electronics in Sensors and Biotechnology*, Mc-Graw-Hill, 2009, ch. 10, pp. 361–394.
25 C. Dhand, S. P. Singh, S. K. Arya, B. Datta and B. D. Malhotra, *Anal. Chim. Acta*, 2007, **602**, 244–251.
26 C. Dhand, S. K. Arya, S. P. Singh, B. P. Singh, M. Datta and B. D. Malhotra, *Carbon*, 2008, **46**, 1727–1735.
27 S. K. Arya, M. Datta, S. P. Singh and B. D. Malhotra, *Anal. Bioanal. Chem.*, 2007, **389**, 2235–2242.
28 R. S. Nicholson and I. Shain, *Anal. Chem.*, 1964, **36**, 706–723.